

Approximate message passing for nonconvex sparse regularization with stability and asymptotic analysis

Ayaka Sakata^{1,2} and Yingying Xu³

¹The Institute of Statistical Mathematics, Midori-cho, Tachikawa 190-8562, Japan

²The Graduate University for Advanced Science (SOKENDAI), Hayama-cho, Kanagawa 240-0193, Japan

³Department of Computer Science, School of Science, Aalto University, P.O.Box 15400, FI-00076 Aalto, Finland

E-mail: ^{1,2}ayaka@ism.ac.jp, ³yingying.xu@aalto.fi

Abstract. We analyze linear regression problem with a nonconvex regularization called smoothly clipped absolute deviation (SCAD) under overcomplete Gaussian basis for Gaussian random data. We develop a message passing algorithm SCAD-AMP and analytically show that the stability condition is corresponding to the AT condition in spin glass literature. As asymptotic analysis, we show the correspondence between density evolution of SCAD-AMP and replica symmetric solution. Numerical experiments confirm that for sufficiently large system size, SCAD-AMP achieves the optimal performance predicted by replica method. From replica analysis, phase transition between replica symmetric (RS) and replica symmetry breaking (RSB) region is found in the parameter space of SCAD. The appearance of RS region for nonconvex penalty is a great advantage which indicate the region of smooth landscape of the optimization problem. Furthermore, we analytically show that the statistical representation performance of SCAD penalty is improved compared with ℓ_1 -based methods, and the minimum representation error under RS assumption is obtained at the edge of RS/RSB phase. The correspondence between the convergence of the existing coordinate descent algorithm and RS/RSB transition is also indicated.

1. Introduction

Variable selection is a basic and important problem in statistics, in which the goal is to find parameters that is significant for the description of given data and prediction of unknown data. The sparse estimation approach for variable selection in high-dimensional statistical modeling, which has the advantage of computational efficiency, stability, and to draw sampling properties compare with traditional approaches follow stepwise and subset selection procedures [1], has been intensively studied for the recent decades. The trends of the sparse estimation is accelerated after the proposing of the LASSO [2], where the variable selection is formulated as a convex problem of the minimization of loss function associated with ℓ_1 regularization. Although LASSO has many attractive properties, the shrinkage introduced by the LASSO results in significant

bias toward 0 for large regression coefficients. To resolve this problem, nonconvex penalties are proposed, such as smoothly clipped absolute deviation (SCAD) penalty, and minimax concave penalty (MCP) [3]. The estimators under these regularizations have all of the desirable properties, including unbiasedness, sparsity, and continuity [4]. The nonconvex penalties are seemingly hard to tackle because of the concerns about local minima due to lack of convexity, and hence the development of efficient algorithms and verification of its typical performance has not been achieved. In earlier studies, it is shown that coordinate descent (CD) is one of the efficient algorithms for these nonconvex penalties. A sufficient condition in parameter space for CD to converge to the globally stable state has been proposed in [5], which was derived by satisfy convexity of the objective function in local region of the parameter space that contains the sparse solutions, but the convergence condition is not mathematically derived. Even the optimal potential of the nonconvex sparse penalty was not clear, the existence of such workable region implies that the theoretical method applied to the convex penalty is partially valid for the nonconvex penalty. That gives us the motivation to accomplish the tasks of theoretical evaluation of the performance and development of algorithm with theoretical guarantees which achieves the potential of the nonconvex sparse penalty.

In this paper, we develop an approximate message passing (AMP) algorithm for linear regression with nonconvex regularization. For the comparison with the ℓ_1 penalty, we employ SCAD penalty where the nonconvexity is controlled by parameters and ℓ_1 regularization is contained at a limit of the parameters. We start with a brief review of feature of SCAD penalty in the context of variable selection in the following subsections.

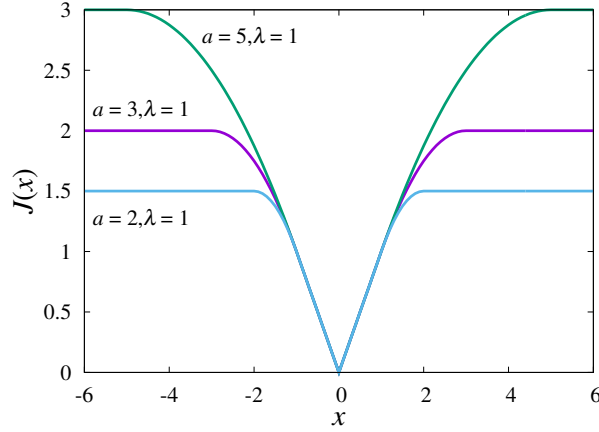
1.1. Overview of variable selection by sparse regularizations

The regularization functions that bring the following properties to the resulting estimator are regarded as appropriate for variable selection [4].

- Unbiasedness:
To avoid excessive modeling bias, the resulting estimator is nearly unbiased when the true unknown parameter is sufficiently large.
- Sparsity:
The resulting estimator should obey a thresholding rule that sets small estimated coefficients to zero and reduces model complexity.
- Continuity:
The resulting estimator should be continuous with respect to data to avoid the instability in model prediction.

Table 1 summarize the properties of the representative regularizations. The regression problem with ℓ_q regularization is called a bridge regression [6]. A well known example for $q > 1$ is ridge regression associated with ℓ_2 penalty [7]. The resulting estimator under ℓ_q ($q > 1$) has continuity, but it is not sparse, and hence ℓ_q ($q > 1$) regularization is not appropriate for the variable selection. ℓ_1 regularization gives a

Regularization	Unbiasedness	Sparsity	Continuity
ℓ_q ($q > 1$)	\times	\times	\checkmark
ℓ_1	\times	\checkmark	\checkmark
ℓ_q ($q < 1$)	\checkmark	\checkmark	\times
SCAD	\checkmark	\checkmark	\checkmark

Table 1. Properties of representative regularizations.**Figure 1.** Shapes of SCAD regularizations for $a = 2, 3$ and 5 at $\lambda = 1$.

continuous solution that obeys a soft thresholding rule, and is widely used in various problems [2, 8], but, ℓ_1 regularization shrinks the estimator by λ . ℓ_q ($q < 1$) penalty gives sparse and unbiased estimator, but the estimator is discontinuous with respect to data.

1.2. Smoothly clipped absolute deviation

Smoothly clipped absolute deviation (SCAD) is one of the nonconvex regularization that improves ℓ_q penalty to simultaneously achieve unbiasedness, sparsity and continuity. The definition of SCAD regularization is

$$J_{\lambda,a}(x) = \begin{cases} \lambda|x| & (|x| \leq \lambda) \\ -\frac{x^2 - 2a\lambda|x| + \lambda^2}{2(a-1)} & (\lambda < |x| \leq a\lambda) \\ \frac{(a+1)\lambda^2}{2} & (|x| > a\lambda) \end{cases}, \quad (1)$$

where λ and $a(> 1)$ are parameters that control the form of the SCAD regularization. In particular, a contributes to the nonconvexity of the SCAD function. Figure 1 shows a -dependence of the SCAD regularization at $\lambda = 1$. In range $[-\lambda, \lambda]$, SCAD regularization behaves as ℓ_1 regularization, and at the limit $\lambda \rightarrow \infty$, it is reduced to ℓ_1 regularization in all region of x . Above $a\lambda$ and below $-a\lambda$, SCAD regularization corresponds to the ℓ_0 -type regularization in the sense that the regularization has a

constant value. These ℓ_1 and ℓ_0 regions are connected by a quadratic function, by which the estimator continuously shifts between the shrunked ℓ_1 type estimator and the unbiased ℓ_0 type estimator. At the limit $a \rightarrow \infty$, the region $[\lambda, a\lambda]$ and $[-a\lambda, -\lambda]$ become linear with gradient λ and $-\lambda$, respectively, and hence SCAD regularization is reduced to ℓ_1 regularization.

SCAD regularization provides the oracle property to the estimator in the least square problem [4, 9, 10]. In other words, when the true solution exists, the zero components in the true parameters are estimated as 0 with probability tending to 1, and the nonzero components are estimated as well as when the correct support, which is the position of non-zero components, is known. The conditions for the oracle property, which are subject to the true solution and the predictor matrix, and the appropriate scaling of λ with respect to the data dimension are mathematically provided [4].

1.3. Our main contributions

In this paper, we focus on the linear regression problem in high-dimensional setting where target data $\mathbf{y} \in \mathbb{R}^M$ is approximated by using an overcomplete predictor matrix or basis matrix $\mathbf{A} \in \mathbb{R}^{M \times N}$ ($M < N$) as $\mathbf{y} \sim \mathbf{A}\mathbf{x}$. The regression coefficient $\mathbf{x} \in \mathbb{R}^N$ is to be estimated under nonconvex sparse penalty. Among the given overcomplete basis matrix, a small combination of basis vectors is selected corresponding to the regularization parameters, which compactly and accurately represent the target data. The sparse representation under the overcomplete basis is an appropriate problem to check variable selection ability of the sparse regularization.

We describe the organization of this paper and list main contributions:

- We develop an efficient message passing algorithm SCAD-AMP for SCAD regularized linear regression problem (section 3.1), and analytically show its local stability condition in section 3.3.
- As an asymptotic analysis, density evolution of the message passing algorithm is shown in section 3.2. The equivalence of the stability of AMP's fixed point and replica symmetric solution is shown in section 4. The validness of the asymptotic analysis is confirmed by numerical simulation.
- Employing replica method from statistical mechanics, a phase transition between replica symmetric (RS) and replica symmetric breaking (RSB) phase is found in the parameter space of SCAD penalty (section 5). In other words, RS phase is present when the nonconvexity of the regularization is appropriately controlled. We also confirm that the conventional parameter setting $a = 3.7$ corresponds to RS phase for sufficient large λ .
- We show the stability of RS solution corresponds to that of AMP's fixed points. It means that the local stability of AMP is mathematically guaranteed in the RS phase. This correspondence holds irrespective of the kind of regularizations, and hence the result is valid for other regularizations where RS/RSB transition appears (section 4.1).

- We evaluate the statistically optimal value of the error between \mathbf{y} and \mathbf{Ax} for the SCAD regularized linear regression problem. The error has decreasing tendency as parameter a decreases so as to approach to the RS/RSB boundary, and is the lowest at the edge of RS/RSB phase. In addition, we analyze parameter dependence of the density of non-zero components in \mathbf{x} in the RS phase. The sparsity is almostly controlled by λ , but as a decreases, the number of non-zero components slightly increases. ℓ_1 regularization corresponds to $a \rightarrow \infty$ of SCAD regularization, and hence SCAD typically provides more accurate and sparser expression compared with ℓ_1 in RS phase (section 5).
- It is numerically shown that the RS/RSB transition point corresponds to the limit that the coordinate descent algorithm reaches the globally stable solution (section 6).
- Our analysis shows that the transient region of SCAD estimates between ℓ_1 -type and ℓ_0 type contributes to the occurrence of the RSB transition (section 4.1).

2. Problem settings

In this paper, we analyze linear regression problem with SCAD regularization, which is formulated as

$$\min_{\mathbf{x}} \frac{1}{2} \|\mathbf{y} - \mathbf{Ax}\|_2^2 + J_{\lambda,a}(\mathbf{x}), \quad (2)$$

where $\mathbf{y} \in \mathbb{R}^M$ and $\mathbf{A} \in \mathbb{R}^{M \times N}$ are given data and predictor matrix or basis matrix, respectively. Here, we consider the case that the generative model of \mathbf{y} does not contain true sparse expression, and hence (2) corresponds to a compression problem of the given data \mathbf{y} under the basis \mathbf{A} , rather than the reconstruction of the true signal. We assume that each component of \mathbf{y} and \mathbf{A} is independently and identically distributed according to Gaussian distributions. More specifically, their joint distribution is given by

$$P_{\mathbf{y},\mathbf{A}}(\mathbf{y}, \mathbf{A}) = P_{\mathbf{y}}(\mathbf{y})P_{\mathbf{A}}(\mathbf{A}) \quad (3)$$

$$P_{\mathbf{y}}(\mathbf{y}) = \prod_{\mu=1}^M \frac{1}{\sqrt{2\pi\sigma_y^2}} \exp\left(-\frac{y_\mu^2}{2\sigma_y^2}\right) \quad (4)$$

$$P_{\mathbf{A}}(\mathbf{A}) = \prod_{\mu=1}^M \prod_{i=1}^N \sqrt{\frac{M}{2\pi}} \exp\left(-\frac{MA_{\mu i}^2}{2}\right). \quad (5)$$

In conventional analysis by statistical mechanics for linear systems such as compressed sensing problems, the elements of the matrix \mathbf{A} are often assumed with zero mean and variance $1/N$. We set the variance to $1/M$ in order to match the conventional assumptions in statistics literature for $\sum_{\mu} A_{\mu i}^2 = 1$ holds for all i . The coefficient $1/2$ of (2) is introduced for mathematical convenience, and we denote the function to be minimized divided by M as

$$e(\mathbf{x}|\mathbf{y}, \mathbf{A}) \equiv \frac{1}{M} \left\{ \frac{1}{2} \|\mathbf{y} - \mathbf{Ax}\|_2^2 + J_{\lambda,a}(\mathbf{x}) \right\}, \quad (6)$$

which corresponds to the energy density. When the regularization is given by ℓ_1 norm, the problem is known as LASSO [2]. SCAD regularization induces the zero-components into the estimated variable \mathbf{x} corresponding to parameters λ and a . We set λ and a as $O(1)$ irrespective of the system size.

We introduce the posterior distribution of the estimate with a parameter β

$$P_\beta(\mathbf{x}|\mathbf{y}, \mathbf{A}) = \exp \{-\beta M e(\mathbf{x}|\mathbf{y}, \mathbf{A}) - \ln Z_\beta(\mathbf{y}, \mathbf{A})\}, \quad (7)$$

where $Z_\beta(\mathbf{y}, \mathbf{A})$ is the normalization constant. The limit $\beta \rightarrow \infty$ leads the uniform distribution over the minimizers of (2). Estimate of the solution of (2) under a fixed set of $\{\mathbf{y}, \mathbf{A}\}$, denoted by $\hat{\mathbf{x}}(\mathbf{y}, \mathbf{A})$, is given by

$$\hat{\mathbf{x}}(\mathbf{y}, \mathbf{A}) = \lim_{\beta \rightarrow \infty} \langle \mathbf{x} \rangle_\beta, \quad (8)$$

where $\langle \cdot \rangle_\beta$ denotes the expectation according to (7) at β .

We focus on the overcomplete basis, where the number of the column vectors are larger than the dimension of the data: $N > M$ with the compression ratio $\alpha = M/N$ (< 1). We do not impose the orthogonality to the basis vectors. In general, the overcomplete basis gives infinitely large numbers of solutions, but adding the cost functions that promote sparsity, more informative representation than that under the orthogonal basis is sought. The sparse representation under the overcomplete basis is an appropriate problem to check variable selection ability of the sparse regularization.

3. Approximate Message Passing algorithm

Exact computation of the expectation in (8) requires exponential time and is thus intractable [11]. We develop an approximate algorithm for (8) following the framework of belief propagation (BP) or message passing [12, 13, 14, 15]. BP has been developed for problems utilizing sparse regularizations such as compressed sensing with linear measurements [16] and LASSO [17, 18], and showing high reconstruction accuracy and computational efficiency. To incorporate the nonconvex penalty, we employ a variant of BP known as generalized approximate message passing (GAMP) [19]. In the following, we show the details of the derivation of the SCAD-AMP algorithm first, and then provide the asymptotic analysis. Stability analysis will be shown in the end of the section, which is an essential and a common concern for algorithms developed for nonconvex regularizations.

3.1. Derivation of SCAD-AMP

We explain the algorithm from general form to specific form for SCAD penalty. And we clarify the required assumptions on elements of matrix \mathbf{A} in each stage of simplification.

Stage 1: General form of Belief propagation

We graphically denote the probability system by two kinds of nodes, and connect them by an edge when they are related. The conditional probability of y_μ depends

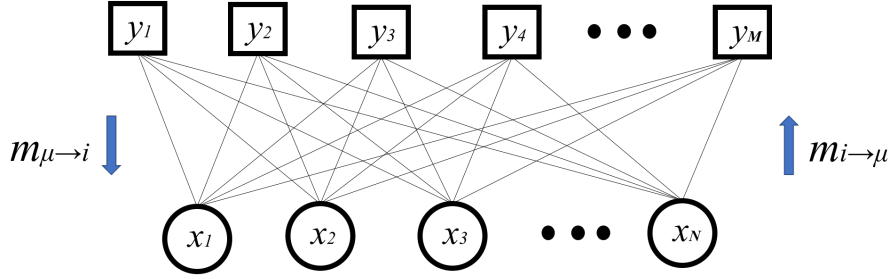


Figure 2. Graphical representation of Belief propagation.

on all x_1, x_2, \dots, x_N , implying that the posterior distribution (7) can be expressed as a (dense) complete bipartite graph, as shown in figure 2. Let us define a general constraint/penalty/prior distribution for the variable nodes as $P_{\text{penalty}}(\mathbf{x})$, and a probability distribution for the output function nodes as $P(\mathbf{y}|\mathbf{A}\mathbf{x})$. The canonical BP equations for the probability $P(\mathbf{x}|\mathbf{A}, \mathbf{y})$ are generally expressed in terms of $2M \times N$ messages, $m_{i \rightarrow \mu}(x_i)$ and $m_{\mu \rightarrow i}(x_i)$ ($i = 1, 2, \dots, N$ and $\mu = 1, 2, \dots, M$), which represent probability distribution functions that carry posterior information and output measurement information, respectively. The messages are written as

$$m_{\mu \rightarrow i}(x_i) = \frac{1}{Z_{\mu \rightarrow i}} \int \prod_{j \neq i} dx_j P(y_\mu | (\mathbf{A}\mathbf{x})_\mu) \prod_{j \neq i} m_{j \rightarrow \mu}(x_j), \quad (9)$$

$$m_{i \rightarrow \mu}(x_i) = \frac{1}{Z_{i \rightarrow \mu}} P_{\text{penalty}}(x_i) \prod_{\gamma \neq \mu} m_{\gamma \rightarrow i}(x_i), \quad (10)$$

where, $Z_{\mu \rightarrow i}$ and $Z_{i \rightarrow \mu}$ are normalization constants to satisfy $\int dx_i m_{\mu \rightarrow i}(x_i) = \int dx_i m_{i \rightarrow \mu}(x_i) = 1$.

Means and variances of x_i under the posterior information message distributions are defined by

$$a_{i \rightarrow \mu} \equiv \int dx_i x_i m_{i \rightarrow \mu}(x_i), \quad (11)$$

$$\nu_{i \rightarrow \mu} \equiv \int dx_i x_i^2 m_{i \rightarrow \mu}(x_i) - a_{i \rightarrow \mu}^2. \quad (12)$$

We also define

$$\omega_\mu \equiv \sum_i A_{\mu i} a_{i \rightarrow \mu}, \quad (13)$$

$$V_\mu \equiv \sum_i A_{\mu i}^2 \nu_{i \rightarrow \mu}, \quad (14)$$

for notational convenience. Using (9), the approximation of marginal distributions (beliefs) are evaluated as

$$m_i(x_i) = \frac{1}{Z_i} P_{\text{penalty}}(x_i) \prod_{\mu=1}^M m_{\mu \rightarrow i}(x_i), \quad (15)$$

where Z_i is a normalization constant for $\int dx_i m_i(x_i) = 1$. We denote the means and variances of the beliefs as a_i and ν_i , which are given by

$$a_i \equiv \int dx_i x_i m_i(x_i) \quad (16)$$

$$\nu_i \equiv \int dx_i x_i^2 m_i(x_i) - a_i^2. \quad (17)$$

The mean $\mathbf{a} = (a_i)$ represents the approximation of the posterior mean $\hat{\mathbf{x}}(\mathbf{y}, \mathbf{A})$.

The coupled integral equations (9) (10) for the messages are too complicated to be of any practical use. However, in the large N, M limit, when the matrix elements $A_{\mu i}$ scale as $1/\sqrt{M}$ (or $1/\sqrt{N}$), these equations can be simplified. We derive algebraic equations corresponding to (9) and (10) using sets of $a_{i \rightarrow \mu}$ and $\nu_{i \rightarrow \mu}$. To do this, we define $u_\mu \equiv (\mathbf{A}\mathbf{x})_\mu$ and inserting the identity

$$\begin{aligned} 1 &= \int du_\mu \delta(u_\mu - (\mathbf{A}\mathbf{x})_\mu) \\ &= \int du_\mu \frac{1}{2\pi} \int d\hat{u}_\mu \exp \left\{ -i\hat{u}_\mu \left(u_\mu - \sum_{i=1}^N A_{\mu i} x_i \right) \right\} \end{aligned} \quad (18)$$

into (9), which yields

$$\begin{aligned} m_{\mu \rightarrow i}(x_i) &= \frac{1}{2\pi Z_{\mu \rightarrow i}} \int du_\mu P(y_\mu | u_\mu) \int d\hat{u}_\mu \exp \left\{ -i\hat{u}_\mu (u_\mu - A_{\mu i} x_i) \right\} \\ &\times \prod_{j \neq i} \left\{ \int dx_j m_{j \rightarrow \mu}(x_j) \exp \left\{ i\hat{u}_\mu A_{\mu j} x_j \right\} \right\}. \end{aligned} \quad (19)$$

We truncate the Taylor series of $\exp\{i\hat{u}_\mu A_{\mu j} x_j\}$ for $j \neq i$ up to the second order of $A_{\mu j}$. Integrating $\int dx_j m_{j \rightarrow \mu}(x_j) (\dots)$ for $j \neq i$, and carrying out the resulting Gaussian integral of \hat{u}_μ , we obtain

$$\begin{aligned} m_{\mu \rightarrow i}(x_i) &= \frac{1}{Z_{\mu \rightarrow i} \sqrt{2\pi(V_\mu - A_{\mu i}^2 \nu_{i \rightarrow \mu})}} \int du_\mu P(y_\mu | u_\mu) \\ &\times \exp \left\{ -\frac{(u_\mu - \omega_\mu - A_{\mu i}(x_i - a_{i \rightarrow \mu}))^2}{2(V_\mu - A_{\mu i}^2 \nu_{i \rightarrow \mu})} \right\}. \end{aligned} \quad (20)$$

We again truncate the Taylor series of the exponential in (20) up to the second order on ground of the smallness of $A_{\mu i}$. As a result, a parameterized expression of $m_{\mu \rightarrow i}(x_i)$ is derived as

$$m_{\mu \rightarrow i}(x_i) = \frac{1}{\tilde{Z}_{\mu \rightarrow i}} \exp \left\{ -\frac{\mathcal{A}_{\mu \rightarrow i}}{2} x_i^2 + \mathcal{B}_{\mu \rightarrow i} x_i \right\}, \quad (21)$$

where $\tilde{Z}_{\mu \rightarrow i} = \sqrt{\frac{2\pi}{\mathcal{A}_{\mu \rightarrow i}}} e^{\frac{\mathcal{B}_{\mu \rightarrow i}^2}{2\mathcal{A}_{\mu \rightarrow i}}}$. The parameters $\mathcal{A}_{\mu \rightarrow i}$ and $\mathcal{B}_{\mu \rightarrow i}$ are evaluated as

$$\mathcal{A}_{\mu \rightarrow i} = (g'_{\text{out}})_\mu A_{\mu i}^2 \quad (22)$$

$$\mathcal{B}_{\mu \rightarrow i} = (g_{\text{out}})_\mu A_{\mu i} + (g'_{\text{out}})_\mu A_{\mu i}^2 a_{i \rightarrow \mu} \quad (23)$$

using

$$(g_{\text{out}})_\mu \equiv \frac{\partial}{\partial \omega_\mu} \log \left(\int du_\mu P(y_\mu | u_\mu) \exp \left(-\frac{(u_\mu - \omega_\mu)^2}{2(V_\mu - A_{\mu i}^2 \nu_{i \rightarrow \mu})} \right) \right) \quad (24)$$

$$(g'_{\text{out}})_\mu \equiv -\frac{\partial^2}{\partial \omega_\mu^2} \log \left(\int du_\mu P(y_\mu | u_\mu) \exp \left(-\frac{(u_\mu - \omega_\mu)^2}{2(V_\mu - A_{\mu i}^2 \nu_{i \rightarrow \mu})} \right) \right). \quad (25)$$

The derivation of these is given in appendix of [20]. Equations (22) and (23) act as the algebraic expression of (9). Note that the form of g_{out} and g'_{out} only depend on the output distribution $P(y_\mu | u_\mu)$. We will give the specific expression of g_{out} , g'_{out} for linear regression later.

A similar expression for (10) is obtained by substituting the last expression of (21) into (10), which leads to

$$m_{i \rightarrow \mu}(x_i) = \frac{1}{\tilde{Z}_{i \rightarrow \mu}} P_{\text{penalty}}(x_i) e^{-\frac{(x_i^2/2) \sum_{\gamma \neq \mu} \mathcal{A}_{\gamma \rightarrow i} + x_i \sum_{\gamma \neq \mu} \mathcal{B}_{\gamma \rightarrow i}}{\tilde{Z}_{i \rightarrow \mu}}}, \quad (26)$$

where $\tilde{Z}_{i \rightarrow \mu}$ is a normalization constant. Expression of equation (26) indicates that $\prod_{\gamma \neq \mu} m_{\gamma \rightarrow i}(x_i)$ in (10) is expressed as a Gaussian distribution with mean $R_{i \rightarrow \mu}$ and variance $\Sigma_{i \rightarrow \mu}^2$ given by

$$R_{i \rightarrow \mu} = \frac{\sum_{\gamma \neq \mu} \mathcal{B}_{\gamma \rightarrow i}}{\sum_{\gamma \neq \mu} \mathcal{A}_{\gamma \rightarrow i}} \quad (27)$$

$$\Sigma_{i \rightarrow \mu}^2 = \left(\sum_{\gamma \neq \mu} \mathcal{A}_{\gamma \rightarrow i} \right)^{-1}. \quad (28)$$

We define an auxiliary distribution of x

$$\mathcal{M}(x; \Sigma^2, R) = \frac{1}{\hat{Z}(\Sigma^2, R)} P_{\text{penalty}}(x) \frac{1}{\sqrt{2\pi\Sigma^2}} \exp \left(-\frac{(x - R)^2}{2\Sigma^2} \right), \quad (29)$$

and the mean and variance over this distribution are defined as functions

$$f_a(\Sigma^2, R) \equiv \int dx x \mathcal{M}(\Sigma^2, R, x), \quad (30)$$

$$f_c(\Sigma^2, R) \equiv \int dx x^2 \mathcal{M}(\Sigma^2, R, x) - f_a^2(\Sigma^2, R). \quad (31)$$

Note, the form of f_a and f_c depend only on distribution $P_{\text{penalty}}(x)$. For a general penalty distribution of x , the functions f_a and f_c are computed by numerical integration over x . In special cases, such as Bernoulli Gaussian or l_1 penalty, these functions are easily computed analytically [20], and SCAD is also the case. We will give the specific analytic form of f_a, f_c for SCAD penalty later.

In (29), $\hat{Z}(\Sigma^2, R)$ is a normalization constant for the distribution and notice that

$$f_a(\Sigma^2, R) = R + \Sigma^2 \frac{\partial}{\partial R} \log \hat{Z}(\Sigma^2, R), \quad (32)$$

$$f_c(\Sigma^2, R) = \Sigma^2 \frac{\partial}{\partial R} f_a(\Sigma^2, R). \quad (33)$$

Referring to the definitions of $a_{i \rightarrow \mu}$ and $\nu_{i \rightarrow \mu}$ in (11) and (12), provide the closed form of BP update as

$$a_{i \rightarrow \mu} = f_a(\Sigma_{i \rightarrow \mu}^2, R_{i \rightarrow \mu}), \quad (34)$$

$$\nu_{i \rightarrow \mu} = f_c(\Sigma_{i \rightarrow \mu}^2, R_{i \rightarrow \mu}), \quad (35)$$

The evaluation of the moments of $m_i(x_i)$ is performed by adding the μ dependent part to (34) and (35) as

$$a_i = f_a(\Sigma_i^2, R_i), \quad (36)$$

$$\nu_i = f_c(\Sigma_i^2, R_i), \quad (37)$$

where

$$\Sigma_i^2 = \left(\sum_{\mu} \mathcal{A}_{\mu \rightarrow i} \right)^{-1} \quad (38)$$

$$R_i = \frac{\sum_{\mu} \mathcal{B}_{\mu \rightarrow i}}{\sum_{\mu} \mathcal{A}_{\mu \rightarrow i}}. \quad (39)$$

Equations (11), (12) together with (22), (23) and (26) lead to closed iterative message passing equations. These equations can be used for any data vector \mathbf{y} and matrix \mathbf{A} . We are considering the case that the matrix \mathbf{A} is not sparse ($\sum_i A_{\mu i} x_i$ contains of order N non-zero terms), and each element of the matrix scales as $O(1/\sqrt{M})$ (or $O(1/\sqrt{N})$). Thanks to this fact, the use of mean and variances instead of the canonical BP messages is exact in the large N limit.

Stage 2: The TAP form of the general message passing algorithm

BP updates $2M \times N$ messages using (22), (23), (34), and (35) for $i = 1, \dots, N$ and $\mu = 1, \dots, M$ in each iteration. The computational cost of this procedure is $O(M^2 \times N + M \times N^2)$ per iteration, which limit the practical utility of BP to systems of relatively small size. In fact, it is possible to rewrite the BP equations in terms of $M + N$ messages instead of $2M \times N$, within the assumption that matrix \mathbf{A} is not sparse and all its elements scale as $O(1/\sqrt{M})$ (or $O(1/\sqrt{N})$). In statistical physics, BP with the reduced messages corresponds to the Thouless-Anderson-Palmer equations (TAP) [21] in the study of spin glasses. For large N , the TAP form are equivalent to the BP equations and it is named the AMP algorithm [16] in compressed sensing. This form will result in a significant reduction of computational complexity to $O(M \times N)$ per iteration which enhanced the practical utility of message passing.

First, for sufficiently large system, $A_{\mu i}^2$ vanishes as $O(M^{-1})$ while $\nu_{i \rightarrow \mu} \sim O(1)$, we ignore $A_{\mu i}^2 \nu_{i \rightarrow \mu}$ in (20). Then we obtain

$$(g_{\text{out}})_{\mu} \equiv \frac{\partial}{\partial \omega_{\mu}} \log \left(\int du_{\mu} P(y_{\mu} | u_{\mu}) \exp \left(-\frac{(u_{\mu} - \omega_{\mu})^2}{2V_{\mu}} \right) \right) \quad (40)$$

$$(g'_{\text{out}})_{\mu} \equiv -\frac{\partial^2}{\partial \omega_{\mu}^2} \log \left(\int du_{\mu} P(y_{\mu} | u_{\mu}) \exp \left(-\frac{(u_{\mu} - \omega_{\mu})^2}{2V_{\mu}} \right) \right), \quad (41)$$

which can be used in Σ_i^2 and R_i :

$$\Sigma_i^2 = \left(\sum_{\mu} (g'_{\text{out}})_{\mu} A_{\mu i}^2 \right)^{-1}, \quad (42)$$

$$R_i = a_i + \left(\sum_{\mu} (g_{\text{out}})_{\mu} A_{\mu i} \right) \Sigma_i^2. \quad (43)$$

In the large N limit, it is clear from (34) and (35) that the messages $a_{i \rightarrow \mu}$ and $\nu_{i \rightarrow \mu}$ are nearly independent of μ . However, one must be careful to keep the correcting terms which are called as the ‘‘Onsager reaction terms’’ [21, 22] in spin glass literature. We express $a_{i \rightarrow \mu}$ by applying Taylor’s expansion to (34) around R_i as

$$\begin{aligned} a_{i \rightarrow \mu} &= f_a \left(\frac{1}{\sum_{\gamma} \mathcal{A}_{\gamma \rightarrow i} - \mathcal{A}_{\mu \rightarrow i}}, \frac{\sum_{\gamma} \mathcal{B}_{\gamma \rightarrow i} - \mathcal{B}_{\mu \rightarrow i}}{\sum_{\gamma} \mathcal{A}_{\gamma \rightarrow i} - \mathcal{A}_{\mu \rightarrow i}} \right) \\ &\simeq a_i + \frac{\partial f_a(\Sigma_i^2, R_i)}{\partial R_i} (-\mathcal{B}_{\mu \rightarrow i} \Sigma_i^2) + O(N^{-1}), \end{aligned} \quad (44)$$

where $\mathcal{B}_{\mu \rightarrow i} \sim O(N^{-1/2})$ and $\sum_{\gamma} \mathcal{A}_{\gamma \rightarrow i} - \mathcal{A}_{\mu \rightarrow i}$ is approximated as $\sum_{\gamma} \mathcal{A}_{\gamma \rightarrow i} = \Sigma_i^{-2}$, because of the smallness of $\mathcal{A}_{\mu \rightarrow i} \propto A_{\mu i}^2 \sim O(M^{-1})$. According to definition (13), multiplying (44) by $A_{\mu i}$ and summing the resultant expressions over i yields

$$\omega_{\mu} = \sum_i A_{\mu i} a_i - (g_{\text{out}})_{\mu} V_{\mu}, \quad (45)$$

where we have used $\nu_i = f_c(\Sigma_i^2, R_i) = \Sigma_i^2 \frac{\partial f_a(\Sigma_i^2, R_i)}{\partial R_i}$.

The computation of V_{μ} is similar, since $\nu_{i \rightarrow \mu}$ is multiplied by $A_{\mu i}^2$, all the correction terms are negligible in the $N \rightarrow \infty$ limit. Therefore, we have

$$V_{\mu} = \sum_i A_{\mu i}^2 \nu_i. \quad (46)$$

The general TAP form of the message passing or general approximated message passing algorithm is summarized in figure 3.

Stage 3: Further simplification for basis matrix with random entries

For special cases of random matrix \mathbf{A} , the TAP equations can be simplified further. For homogeneous matrix \mathbf{A} with i.i.d random entries of zero mean and variance $1/M$ (the distribution can be anything as long as the mean and variance are fixed), the simplification can be understood as follows. Define V as the average of V_{μ} with respect to different realizations of the matrix \mathbf{A} . We replace $\{A_{\mu j}^2\}$ in $V_{\mu} = \sum_i A_{\mu i}^2 \nu_{i \rightarrow \mu}$ with its expectation M^{-1} from the law of large numbers. This replacement makes V_{μ} for any μ equal to their average as

$$V \equiv \sum_{i=1}^N \overline{A_{\mu i}^2} \nu_i = \frac{1}{M} \sum_{i=1}^N \nu_i, \quad (47)$$

where $\overline{\cdots}$ denotes average over $A_{\mu i}$. The same argument can be repeated for all the terms that contain $A_{\mu i}$. For sufficiently large N , Σ_i^2 typically converges to a constant

Algorithm 1: GENERAL APPROXIMATE MESSAGE PASSING($\mathbf{a}^*, \boldsymbol{\nu}^*, \boldsymbol{\omega}^*$)

1) Initialization :

\mathbf{a} seed : $\mathbf{a}_0 \leftarrow \mathbf{a}^*$
 $\boldsymbol{\nu}$ seed : $\boldsymbol{\nu}_0 \leftarrow \boldsymbol{\nu}^*$
 $\boldsymbol{\omega}$ seed : $\boldsymbol{\omega}_0 \leftarrow \boldsymbol{\omega}^*$
Counter : $t \leftarrow 0$

2) Counter increase :

$t \leftarrow t + 1$

3) Mean of variances of posterior information message distributions :

$V_\mu^{(t)} \leftarrow (\sum_i A_{\mu i}^2 \nu^{(t-1)})$

4) Self-feedback cancellation :

$\omega_\mu^{(t)} \leftarrow \sum_i A_{\mu i} a_i^{(t-1)} - V_\mu^{(t-1)} g_{\text{out}}(\omega_\mu^{(t-1)}, V_\mu^{(t-1)})$

5) Variances of output information message distributions :

$(\Sigma_i^2)^{(t)} \leftarrow \left(\sum_\mu A_{\mu i}^2 g'_{\text{out}}(\omega_\mu^{(t)}, V_\mu^{(t)}) \right)^{-1}$

6) Average of output information message distributions :

$R_i^{(t)} \leftarrow a_i^{(t-1)} + \left(\sum_\mu A_{\mu i} g_{\text{out}}(\omega_\mu^{(t)}, V_\mu^{(t)}) \right) (\Sigma_i^2)^{(t)}$

7) Posterior mean :

$a_i^{(t)} \leftarrow f_a((\Sigma_i^2)^{(t)}, R_i^{(t)})$

8) Posterior variance :

$\nu_i^{(t)} \leftarrow f_c((\Sigma_i^2)^{(t)}, R_i^{(t)})$

9) Iteration : Repeat from step 2 until convergence.

Figure 3. GAMP algorithm with the assumption that matrix \mathbf{A} is not sparse and all its elements scales as $O(1/\sqrt{M})$ (or $O(1/\sqrt{N})$). The convergent vectors of $\mathbf{a}^{(t)}$, $\boldsymbol{\nu}^{(t)}$ and $\boldsymbol{\omega}^{(t)}$ obtained in the previous loop are denoted by \mathbf{a}^* , $\boldsymbol{\nu}^*$, and $\boldsymbol{\omega}^*$, respectively.

denoted by Σ^2 , independent of index i . This removing of site dependence, in conjunction with (22) and (23), yields

$$\Sigma^2 = \left(\frac{1}{M} \sum_\mu g'_{\text{out}}(\omega_\mu, V) \right)^{-1}, \quad (48)$$

$$R_i = \left(\sum_\mu g_{\text{out}}(\omega_\mu, V) A_{\mu i} \right) \Sigma^2 + a_i. \quad (49)$$

Iterating (47), (48), (49) and

$$\omega_\mu = \sum_i A_{\mu i} a_i - g_{\text{out}}(\omega_\mu, V) V, \quad (50)$$

$$a_i = f_a(\Sigma^2, R_i), \quad (51)$$

$$\nu_i = f_c(\Sigma^2, R_i), \quad (52)$$

we can solve the equations with only $2(M + N + 1)$ variables involved.

SCAD-AMP for linear regression

In this paper, we are considering the case that matrix \mathbf{A} contains i.i.d random variables from zero mean and variance $1/M$ Gaussian distribution. We can employ the simplified version of GAMP algorithm derived above.

First, let us look at the output channel. In linear regression problem,

$$P(y_\mu | u_\mu) = \exp \left\{ -\frac{\beta}{2} (y_\mu - u_\mu)^2 \right\} \quad (53)$$

where we concentrate our analysis on $\beta \rightarrow \infty$ case. We re-scale $\tilde{V} = \beta V$ and $\tilde{\Sigma}^2 = \beta \Sigma^2$ so that \tilde{V} and $\tilde{\Sigma}^2$ are $O(1)$ in the $\beta \rightarrow \infty$ limit. Inserting (53) into (40) and (41) gives $(g_{\text{out}})_\mu$ and $(g'_{\text{out}})_\mu$ as $(g_{\text{out}})_\mu = \beta \frac{y_\mu - \omega_\mu}{\tilde{V} + 1}$ and $(g'_{\text{out}})_\mu = \beta \frac{1}{\tilde{V} + 1}$, respectively. For scaling convenience, we employ

$$(\tilde{g}_{\text{out}})_\mu = \frac{y_\mu - \omega_\mu}{\tilde{V} + 1}, \quad (54)$$

$$(\tilde{g}'_{\text{out}})_\mu = \frac{1}{\tilde{V} + 1}, \quad (55)$$

as function $(g_{\text{out}})_\mu$ and $(g'_{\text{out}})_\mu$ in the general form of GAMP. Inserting (54) to (50) gives

$$\omega_\mu = \sum_i A_{\mu i} a_i - \frac{\tilde{V}}{\tilde{V} + 1} (y_\mu - \omega_\mu), \quad (56)$$

and inserting (55) to (48), we obtain

$$\tilde{\Sigma}^2 = \tilde{V} + 1. \quad (57)$$

Next, on the prior distribution side, inserting SCAD penalty distribution

$$P_{\text{penalty}}(x) = e^{-\beta J_{\lambda, a}(x)}, \quad (58)$$

into (29), in the limit of $\beta \rightarrow \infty$ we obtain

$$\begin{aligned} \hat{Z}(\Sigma^2, R) &= \int_{-\infty}^{\infty} \sqrt{\frac{\beta}{2\pi\tilde{\Sigma}^2}} \exp \left\{ -\beta J_{\lambda, a}(x) - \beta \frac{(x - R)^2}{2\tilde{\Sigma}^2} \right\} dx \\ &= \sqrt{\frac{\beta}{2\pi\tilde{\Sigma}^2}} \exp \left\{ -\beta \phi^*(\tilde{\Sigma}^2, R) \right\}. \end{aligned} \quad (59)$$

where

$$\phi^*(\tilde{\Sigma}^2, R) = \min_x \phi(x; \tilde{\Sigma}^2, R), \quad (60)$$

$$\phi(x; \tilde{\Sigma}^2, R) = J_{\lambda, a}(x) + \frac{(x - R)^2}{2\tilde{\Sigma}^2}, \quad (61)$$

and R is given by inserting (54) and (57) into (49) which gives

$$R_i = \sum_{\mu} A_{\mu i} (y_\mu - \omega_\mu) + a_i. \quad (62)$$

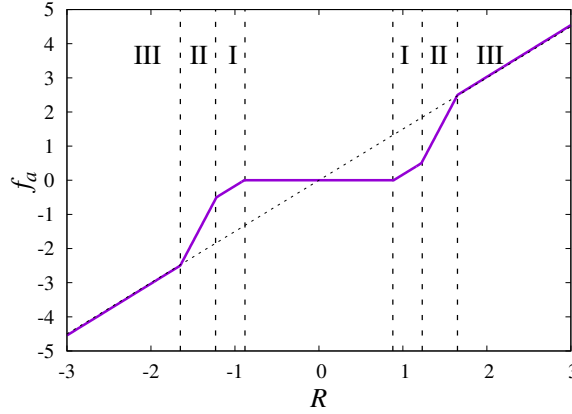


Figure 4. An example of f_a as a function of R . The dashed diagonal line represents the behavior of the estimate when the regularization term does not exist.

At $\beta \rightarrow \infty$, the function f_a corresponds to the minimizer of ϕ as

$$f_a(\Sigma^2, R) = \arg \min_x \phi(x; \tilde{\Sigma}^2, R). \quad (63)$$

Solving the minimization problem, we obtain

$$f_a(\tilde{\Sigma}^2, R) = \tilde{\Sigma}^2 \left(\frac{R}{\tilde{\Sigma}^2} - \lambda \text{sign} \left(\frac{R}{\tilde{\Sigma}^2} \right) \right) \cdot \text{I} \\ + \frac{1}{\frac{1}{\tilde{\Sigma}^2} - \frac{1}{a-1}} \left(\frac{R}{\tilde{\Sigma}^2} - \frac{a}{a-1} \lambda \text{sign} \left(\frac{R}{\tilde{\Sigma}^2} \right) \right) \cdot \text{II} + R \cdot \text{III}, \quad (64)$$

$$f_c(\tilde{\Sigma}^2, R) = \tilde{\Sigma}^2 \cdot \text{I} + \frac{1}{\frac{1}{\tilde{\Sigma}^2} - \frac{1}{a-1}} \cdot \text{II} + \tilde{\Sigma}^2 \cdot \text{III}. \quad (65)$$

where

$$\text{I} = \Theta(|R| > \lambda \tilde{\Sigma}^2) \Theta(|R| \leq \lambda(1 + \tilde{\Sigma}^2)), \quad (66)$$

$$\text{II} = \Theta(|R| > \lambda(1 + \tilde{\Sigma}^2)) \Theta(|R| \leq a\lambda), \quad (67)$$

$$\text{III} = \Theta(|R| > a\lambda). \quad (68)$$

Here we have replaced $f_a(\Sigma^2, R)$ and $f_c(\Sigma^2, R)$ with $f_a(\tilde{\Sigma}^2, R)$ and $f_c(\tilde{\Sigma}^2, R)$, respectively, since there is no β dependence in the final form of (64) and (65). Figure 4 shows an example of f_a as a function of R . In the region I and III, f_a behaves like the ℓ_1 and ℓ_0 estimates, respectively. The estimate in region III is not biased despite the existence of regularization, and hence this region contributes to the unbiasedness of the estimates under SCAD regularization. In region II, f_a transits linearly between the ℓ_1 and ℓ_0 estimates. We will discuss the contribution of this region to the instability of AMP in connection with replica method in Sec.4.

We term the entire procedure as Approximate Message Passing for smoothly clipped absolute deviation (SCAD-AMP) algorithm. Figure 5 shows the pseudocode of SCAD-AMP. To improve the convergence property, employing an appropriate damping factor in conjunction with a normalization of $|\mathbf{a}|$ is valid. The most time-consuming parts of

SCAD-AMP are the matrix-vector multiplications $\sum_{\mu} (g_{\text{out}})_{\mu} A_{\mu i}$ in (43) and $\sum_i A_{\mu i} a_i$ in (45), and hence the computational complexity is $O(NM)$ per iteration. We note that a_i in equation (49) and $(g_{\text{out}})_{\mu} V$ in equation (50) correspond to the *Onsager reaction term* in the spin glass literature [21, 22]. These terms effectively cancel the self-feedback effects, that works to stabilize the convergence of SCAD-AMP.

Algorithm 2: APPROXIMATE MESSAGE PASSING FOR SCAD($\mathbf{a}^*, \boldsymbol{\nu}^*, \boldsymbol{\omega}^*$)

1) Initialization :

aseed : $\mathbf{a}_0 \leftarrow \mathbf{a}^*$
 ν seed : $\boldsymbol{\nu}_0 \leftarrow \boldsymbol{\nu}^*$
 ω seed : $\boldsymbol{\omega}_0 \leftarrow \boldsymbol{\omega}^*$
Counter : $t \leftarrow 0$

2) Counter increase : $t \leftarrow t + 1$
3) Mean of variances of posterior information message distributions :

$$V^{(t)} \leftarrow \mathbf{M}^{-1}(\text{sum}(\boldsymbol{\nu}^{(t-1)}))$$

4) Self-feedback cancellation :

$$\boldsymbol{\omega}^{(t)} \leftarrow \mathbf{A}\mathbf{a}^{(t-1)} - \frac{V^{(t)}}{V^{(t)}+1}(\mathbf{y} - \boldsymbol{\omega}^{(t-1)})$$

5) Average of output information message distributions :

$$(\mathbf{R})^{(t)} \leftarrow \mathbf{a}^{(t-1)} + \mathbf{A}(\mathbf{y} - \boldsymbol{\omega}^{(t)})$$

6) Posterior mean :

$$\hat{\mathbf{a}}^{(t)} \leftarrow f_a((V^{(t)} + 1)\mathbf{1}, \mathbf{R}^{(t)})$$

7) Posterior variance :

$$\hat{\boldsymbol{\nu}}^{(t)} \leftarrow f_c((V^{(t)} + 1)\mathbf{1}, \mathbf{R}^{(t)})$$

8) Iteration : Repeat from step 2 until convergence.

Figure 5. Pseudocode for SCAD-AMP with the assumption that matrix \mathbf{A} contains i.i.d random variables with zero mean and variance $1/M$. For linear regression problem, the variance vector of output information message distributions is $\mathbf{V} + \mathbf{1}$. Function f_a and f_c for SCAD are (64) and (65), respectively. The convergent vectors of $\mathbf{a}^{(t)}$, $\boldsymbol{\nu}^{(t)}$ and $\boldsymbol{\omega}^{(t)}$ obtained in the previous loop are denoted by \mathbf{a}^* , $\boldsymbol{\nu}^*$, and $\boldsymbol{\omega}^*$, respectively. $\mathbf{1}$ is the N -dimensional vector whose entries are all unity.

The quantities we are focusing on are calculated at AMP's fixed point. As an example, we calculate the fraction of non-zero components to data dimension, called sparsity,

$$\frac{\rho}{\alpha} = \frac{1}{M} \sum_{i=1}^N |\hat{x}_i|_0, \quad (69)$$

at AMP's fixed point. Figure 6 shows λ -dependence of ρ/α for $N = 200$ and $a = 5$ by circle \circ . The results are averaged over 1000 samples of \mathbf{y} and \mathbf{A} . At a certain value of λ that depends on a , AMP does not converge to fixed points, which values of λ are

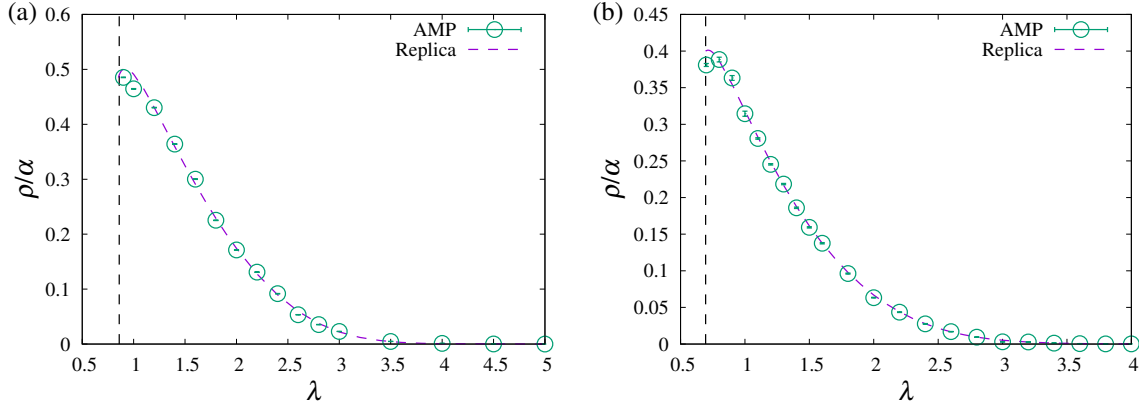


Figure 6. λ dependence of ρ at SCAD-AMP's fixed point for $a = 5$ with (a) $\alpha = 0.1$ and (b) $\alpha = 0.5$. Circles are obtained by SCAD-AMP algorithm. The dashed magenta lines represent SCAD-AMP's convergence limit obtained by replica method, and SCAD-AMP does not converge in the left-hand region of the black dashed lines.

denoted by vertical black dashed lines in Figure 6. For the understanding and practical implement of AMP, the stability analysis of the fixed point is required. We note that the dashed magenta lines in Figure 6 are the results obtained by replica method that describes the asymptotic behavior of AMP, which is explained in Sec.4.

3.2. Macroscopic analysis: density evolution of the message passing

Density evolution is a framework for analyzing the dynamical behaviour of BP pursuing a macroscopic distribution of messages [23]. Here we derive density evolution for linear regression with SCAD penalty in the case where the matrix \mathbf{A} and vector \mathbf{y} have random entries that are i.i.d., with mean 0, variance $1/M$ and σ_y^2 , respectively. We start from the following expression of the quantity $R_i^{(t)}$

$$R_i^{(t)} = \frac{1}{\sum_{\mu} A_{\mu i}^2} \sum_{\mu} \{A_{\mu i} y_{\mu} - A_{\mu i} \sum_{j \neq i} A_{\mu j} a_{j \rightarrow \mu}^{(t)}\}, \quad (70)$$

here the superscript (t) denotes the values at iteration step t . The variables $\{R_i^{(t)}\}$ are random variables with respect to the distribution of the basis matrix elements $A_{\mu i}$ and the data elements y_{μ} , and hence they are regarded as Gaussian random variables from central limit theorem. The mean of $R_i^{(t)}$ is given by

$$\begin{aligned} \overline{R_i^{(t)}} &= \frac{1}{\sum_{\mu} A_{\mu i}^2} \left\{ \sum_{\mu} A_{\mu i} y_{\mu} - \sum_{\mu} \sum_{j \neq i} A_{\mu i} A_{\mu j} a_{j \rightarrow \mu}^{(t)} \right\} \\ &\simeq \sum_{\mu} \overline{A_{\mu i} y_{\mu}} - \sum_{\mu} \sum_{j \neq i} \overline{A_{\mu i} A_{\mu j} a_{j \rightarrow \mu}^{(t)}} = 0, \end{aligned} \quad (71)$$

where $\overline{\cdots}$ denotes the average with respect to \mathbf{A} and \mathbf{y} . The variance of $R_i^{(t)}$, defined as $E^{(t)}$ is given by

$$\begin{aligned} \overline{(R_i^{(t)})^2} &\simeq \overline{\left\{ \sum_{\mu} A_{\mu i} y_{\mu} - \sum_{\mu} \sum_{j \neq i} A_{\mu i} A_{\mu j} a_{j \rightarrow \mu}^{(t)} \right\}^2} \\ &\simeq \sigma_y^2 + \frac{1}{M} \sum_{j=1}^N \overline{(a_j^{(t)})^2} \equiv E^{(t)}, \end{aligned} \quad (72)$$

where we neglected terms of $O(1/\sqrt{N})$. Using the statistical property of $R_i^{(t)}$, the marginal distribution at iteration $t+1$ denoted by $m_i^{(t+1)}(x_i)$ is distributed as

$$m_i^{(t+1)}(x_i) \simeq \frac{1}{\hat{Z}_i^{(t+1)}} P_{\text{penalty}}(x_i) \exp \left\{ -\beta \frac{(x_i - z\sqrt{E^{(t)}})^2}{2(1 + V^{(t)})} \right\}, \quad (73)$$

where z is a random Gaussian variable with zero mean and unit variance, and $\hat{Z}_i^{(t+1)}$ is a normalization constant of the marginal distribution at step $t+1$.

Equation (73) means that the marginal distribution at step t can be simply expressed in terms of two parameters $V^{(t)}$ and $E^{(t)}$ at sufficiently large N . Finally, referring to (30), (31) and definition of E (72), the density evolution equations are derived as

$$V^{(t+1)} = \frac{1}{\alpha} \int Dz f_c(1 + V^{(t)}, z\sqrt{E^{(t)}}), \quad (74)$$

$$E^{(t+1)} = \frac{1}{\alpha} \int Dz f_a^2(1 + V^{(t)}, z\sqrt{E^{(t)}}) + \sigma_y^2, \quad (75)$$

where $\int Dz = \int_{-\infty}^{\infty} \frac{dz}{\sqrt{2\pi}} e^{-z^2/2}$. They describe how macroscopic parameters E and V evolve during the iterations of the BP algorithm. The density evolution equations are the same for the message passing and for the TAP equations as indeed factors of $O(1/N)$ are neglected in the density evolution. The correspondence between density evolution and replica symmetric solution is provided in section 4.

In the current problem setting, the fixed point of the density evolution equation is unique within the range we observed, for any system parameters α , a , and λ .

3.3. Microscopic stability of AMP

Even when the density evolution (74) and (75) converges to a stationary state, the convergence of the microscopic variables updated in AMP such as $R_{i \rightarrow \mu}^t$ is not guaranteed. We perform the linear stability analysis of AMP's fixed points to examine the local stability of AMP's fixed points, which is a necessary condition for the global stability. Similar analysis was also described in [24] for binary signals, here we provide a more general analysis.

The update of $R_{i \rightarrow \mu}^t$ is linearized around a fixed point solution $R_{i \rightarrow \mu}$ using equation (44), yielding

$$R_{i \rightarrow \mu}^{(t+1)} = \frac{1}{\sum_{\gamma \neq \mu} \mathcal{A}_{\gamma \rightarrow i}^t} \left\{ \sum_{\gamma \neq \mu} \frac{A_{\gamma i} y_{\mu} - A_{\gamma i} \sum_{j \neq i} A_{\gamma j} a_j}{V_{\mu} + 1} \right\}$$

$$+ \sum_{\gamma \neq \mu} \frac{A_{\gamma i} \sum_{j \neq i} A_{\gamma j} \frac{\partial f_a(\Sigma_i^2, R_i)}{\partial R}}{V_\mu + 1} R_{j \rightarrow \gamma}^{(t)}. \quad (76)$$

Therefore,

$$\delta R_{i \rightarrow \mu}^{(t+1)} = \frac{1}{V+1} \sum_{\gamma \neq \mu} A_{\gamma i} \sum_{j \neq i} A_{\gamma j} \frac{\partial f_a(\Sigma_i^2, R_i)}{\partial R} \delta R_{j \rightarrow \gamma}^{(t)}, \quad (77)$$

where we have replaced V_μ with the average V and used the assumption that M is large. The summation including the basis matrix elements $\{A_{\mu i}\}$, which are i.i.d. random numbers, on the right-hand side of (77) leads a Gaussian random number, because of the central limit theorem assuming that $\delta R_{i \rightarrow \mu}^t$ are uncorrelated. Furthermore, correlations of $R_{i \rightarrow \mu}^{t+1}$ with respect to indices μ, i and t are negligible, because the right-hand side of (77) does not contain the indices μ and i . These fact makes it possible to analyze the stability of the fixed point by observing the growth of the first and second moments of $\delta R_{i \rightarrow \mu}^t$ through each update.

The first moment of $\delta R_{i \rightarrow \mu}^{(t)}$ is negligible at sufficiently large M and N , since the average of $A_{\mu i}$ is zero. The second moment of $\delta R_{i \rightarrow \mu}^{(t)}$ is given by

$$\begin{aligned} (\delta R_{i \rightarrow \mu}^{(t+1)})^2 &\simeq \frac{1}{(V+1)^2} \overline{\left(\sum_{\gamma \neq \mu} A_{\gamma i} \sum_{j \neq i} A_{\gamma j} \frac{\partial f_a(\Sigma_i^2, R_i)}{\partial R} \delta R_{j \rightarrow \gamma}^{(t)} \right)^2} \\ &= \frac{1}{\alpha(V+1)^2} \frac{1}{M} \sum_{\gamma \neq \mu} \left(\frac{1}{N} \sum_{j \neq i} \overline{\left(\frac{\partial f_a(\Sigma_i^2, R_i)}{\partial R} \right)^2 (\delta R_{j \rightarrow \gamma}^{(t)})^2} \right) \\ &\simeq \frac{1}{\alpha(V+1)^2} \frac{1}{M} \sum_{\gamma \neq \mu} \left(\frac{1}{N} \sum_{j \neq i} \overline{\left(\frac{\partial f_a(\Sigma_i^2, R_i)}{\partial R} \right)^2} \right) \left(\frac{1}{N} \sum_{j \neq i} \overline{(\delta R_{j \rightarrow \gamma}^{(t)})^2} \right) \end{aligned} \quad (78)$$

where we assume the self-averaging property and $\overline{\cdots}$ denotes average over $A_{\mu i}$ and we replaced sample average of products with a product of sample average in the last step, which is valid when N is large. Further, it can be expected that due to the self-averaging property, the macroscopic variable $\overline{\left(\frac{\partial f_a(\Sigma_i^2, R_i)}{\partial R} \right)^2}$ can be expressed as

$$\overline{\left(\frac{\partial f_a(\Sigma_i^2, R_i)}{\partial R} \right)^2} \simeq \int \mathrm{D}z \left(\frac{\partial f_a(V+1, z\sqrt{E})}{\partial(z\sqrt{E})} \right)^2 \quad (79)$$

independent of i , where V and E are a fixed point values of V^t and E^t . For sufficiently large M and N , $N^{-1} \sum_{j \neq i} (\delta R_{j \rightarrow \gamma}^{(t)})^2$ coincides with $(\delta R_{i \rightarrow \mu}^{(t)})^2$ itself, because their dependency on μ can be ignored. Therefore, the second moment is enlarged through the belief update and the fixed point solution becomes locally unstable if

$$\frac{1}{\alpha(V+1)^2} \int \mathrm{D}z \left(\frac{\partial f_a(V+1, z\sqrt{E})}{\partial(z\sqrt{E})} \right)^2 > 1. \quad (80)$$

We will show the correspondence of the AMP's local stability condition and de Almeida-Thouless condition derived from replica method in section 4.

4. Replica analysis

Replica method provides the performance of an optimal algorithm for problem (2). Asymptotic property of AMP's fixed point presented in the previous section can also be analytically derived independently using the replica method. The replica method provides the physical meanings of the density evolution and the stability of AMP. The basis for the analysis is the free energy density defined by

$$f = - \lim_{\beta \rightarrow \infty} \frac{1}{M\beta} E_{\mathbf{y}, \mathbf{A}} [\ln Z_\beta(\mathbf{y}, \mathbf{A})], \quad (81)$$

that corresponds to the expectation of the minimum value of the energy $e(\mathbf{x}|\mathbf{y}, \mathbf{A})$.

The expectation according to (3) is implemented by replica method based on the following identity;

$$E_{\mathbf{y}, \mathbf{A}} [\ln Z_\beta(\mathbf{y}, \mathbf{A})] = \lim_{n \rightarrow 0} \frac{E_{\mathbf{y}, \mathbf{A}} [Z_\beta^n(\mathbf{y}, \mathbf{A})] - 1}{n}, \quad (82)$$

which is employed for the analysis of sparse regularizations in various problems [25, 26, 27, 28]. We briefly summarize the replica analysis for the SCAD penalty. The detailed explanation is shown in Appendix A.

We focus on the $N \rightarrow \infty$ and $M \rightarrow \infty$ limit keeping $M/N = \alpha \sim O(1)$. Under the replica symmetric (RS) assumption, the free energy density is given by

$$f = \text{extr}_{Q, \chi, \hat{Q}, \hat{\chi}} \left\{ \frac{\alpha(Q + \sigma_y^2)}{2(1 + \chi)} - \frac{\alpha(Q\hat{Q} - \chi\hat{\chi})}{2} + \frac{1}{2}\xi(\hat{Q}, \hat{\chi}) \right\}, \quad (83)$$

where $\text{extr}_{Q, \chi, \hat{Q}, \hat{\chi}}$ denotes extremization with respect to the variables $\{Q, \chi, \hat{Q}, \hat{\chi}\}$, which are given by

$$Q = \frac{1}{\alpha} \frac{\partial \xi}{\partial \hat{Q}} \quad (84)$$

$$\chi = -\frac{1}{\alpha} \frac{\partial \xi}{\partial \hat{\chi}} \quad (85)$$

$$\hat{Q} = \frac{1}{1 + \chi} \quad (86)$$

$$\hat{\chi} = \frac{Q + \sigma_y^2}{(1 + \chi)^2} \quad (87)$$

at the extremum. The function $\xi(\hat{Q}, \hat{\chi})$ is given by

$$\xi(\hat{Q}, \hat{\chi}) = 2 \int Dz f_\xi(\sqrt{\hat{\chi}}z, \hat{Q}) \quad (88)$$

$$f_\xi(\sqrt{\hat{\chi}}z, \hat{Q}) = \min_x \left(\frac{\hat{Q}}{2} x^2 - \sqrt{\hat{\chi}}zx + J_{\lambda, a}(x) \right), \quad (89)$$

where $\sqrt{\hat{\chi}}z$ is the random field that effectively represents the randomness introduced by \mathbf{y} and \mathbf{A} . It is shown that Q and χ relate to the physical quantities at the extremum as

$$Q = \lim_{M \rightarrow \infty} \frac{1}{M} \hat{\mathbf{x}}^T \hat{\mathbf{x}} \quad (90)$$

$$\chi = \lim_{\beta \rightarrow \infty} \lim_{M \rightarrow \infty} \frac{\beta}{M} \sum_{i=1}^N (\langle x_i^2 \rangle_\beta - \langle x_i \rangle_\beta^2), \quad (91)$$

where T in superscript means matrix transopose. The solution of x concerned with the effective single-body problem (89), denoted by $x^*(z; \hat{Q}, \hat{\chi})$ for SCAD regularization is given by

$$x^*(z; \hat{Q}, \hat{\chi}) = \frac{\sqrt{\hat{\chi}}z - \lambda \text{sign}(z)}{\hat{Q}} \text{I} + \frac{\sqrt{\hat{\chi}}z - \frac{a\lambda}{a-1} \text{sign}(z)}{\hat{Q} - (a-1)} \text{II} + \frac{\sqrt{\hat{\chi}}z}{\hat{Q}} \text{III} \quad (92)$$

where

$$\text{I} = \Theta(|z| > \sqrt{2}\theta_1) \Theta(|z| \leq \sqrt{\theta_2}) \quad (93)$$

$$\text{II} = \Theta(|z| \geq \sqrt{2}\theta_2) \Theta(|z| < \sqrt{2}\theta_3) \quad (94)$$

$$\text{III} = \Theta(|z| \geq \sqrt{2}\theta_3), \quad (95)$$

and thresholds are given by $\theta_1 = \lambda/\sqrt{2\hat{\chi}}$, $\theta_2 = \lambda(\hat{Q} + 1)/\sqrt{2\hat{\chi}}$, and $\theta_3 = a\lambda\hat{Q}/\sqrt{2\hat{\chi}}$, respectively. The behavior of x^* is the same as Figure 4. Using x^* , the quantities Q and χ in replica method are represented as

$$Q = \frac{1}{\alpha} \int Dz (x^*)^2 \quad (96)$$

$$\chi = \frac{1}{\alpha} \int Dz \frac{\partial x^*}{\partial (\sqrt{\hat{\chi}}z)}. \quad (97)$$

The solution x^* is statistically equivalent to the solution of the original problem (2), and hence the density of non-zero component is given by

$$\rho = \text{erfc}(\theta_1), \quad (98)$$

where $\text{erfc}(\theta) = \frac{2}{\sqrt{\pi}} \int_{\theta}^{\infty} dz \exp(-z^2)$. The dependence of ρ/α on λ derived by replica method is shown in Figure 6 by dashed lines. The results by replica method matches to that by AMP for sufficiently large system size, which is mathematically supported by considering the correspondence between variables used in AMP and replica method.

Comparing f_a in AMP (63) and x^* in replica (89), they are equivalent to each other using the correspondences

$$\Sigma^2 \leftrightarrow \hat{Q}^{-1}, \quad (99)$$

$$R_i/\Sigma^2 \leftrightarrow \sqrt{\hat{\chi}}z. \quad (100)$$

From equations (57) and (86), the correspondence (99) is equivalent to that between V in AMP and χ in replica analysis. It is consistent with the definition of V and the physical meaning of χ given by (91). (100) means that the distribution of R_i/Σ^2 with respect to \mathbf{y} and \mathbf{A} is represented by Gaussian distribution with variance $\hat{\chi}$. From the calculation explained in Appendix A, it is shown that $\hat{\chi}$ corresponds to the representation error defined by

$$\text{err} = \frac{1}{M} E_{\mathbf{y}, \mathbf{A}} [||\mathbf{y} - \mathbf{A}\hat{\mathbf{x}}(\mathbf{y}, \mathbf{A})||_2^2], \quad (101)$$

which evaluate the accuracy of the expression of data using the estimated sparse expression. The variance of R_i is defined as E , and hence

$$E \leftrightarrow \Sigma^2 \hat{\chi} = (1 + V) \hat{\chi} \leftrightarrow (Q + \sigma_y^2) \quad (102)$$

These correspondence means that density evolution (74) and (75) can be regarded as recursively solving the saddle point equations χ and $(Q + \sigma_y^2)$, respectively, under RS assumption.

4.1. de Almeida-Thouless condition for replica symmetric phase

The RS solution discussed thus far loses local stability under perturbations that break the symmetry between replicas in a certain parameter region. Known as de Almeida-Thouless (AT) instability [29], this phenomenon appears when

$$\frac{1}{\alpha(1 + \chi)^2} \int Dz \left(\frac{\partial x^*}{\partial(\sqrt{\chi}z)} \right)^2 > 1 \quad (103)$$

hold [29], as explained in Appendix B. Applying this to the minimizer of the single-body problem (92), we get AT instability condition for SCAD penalty as

$$\frac{\rho}{\alpha} + \left\{ \left(\frac{\hat{Q}}{\hat{Q} - \frac{1}{a-1}} \right)^2 - 1 \right\} \frac{\gamma}{\alpha} > 1, \quad (104)$$

where $\gamma = \text{erfc}(\theta_2) - \text{erfc}(\theta_3)$. At $a \rightarrow \infty$, the AT instability condition for SCAD reduces to that for ℓ_1 regularization: $\rho/\alpha > 1$. The second term of (104) is the characteristics of SCAD regularization. By definition, γ is the probabilistic weight of the transit region (region II of Figure 4), and $\hat{Q}/(\hat{Q} - (a-1)^{-1})$ denotes the ratio between the variances in the transient region and that in other region (equation (92)). Equation (104) means that as the transient region is extended or as the variance of the estimates in the transient region gets smaller, RS solution is likely to be unstable.

Using the correspondence between AMP and RS saddle point discussed so far, AT instability condition (104) coincident with the instability condition of density evolution given by (80). Similar correspondence has been shown in BP algorithm for CDMA [24]. We note that the correspondence between AMP's local stability and RS/RSB transition holds irrespective of the kind of regularizations, and hence the result is valid for other regularizations where RS/RSB transition appears. In the current problem, RS saddle point equation has unique solution; the first order transition does not occur. Therefore, the local stability of the AMP's fixed points indicates the global stability of them.

5. Phase diagram and representation error

Figure 7 shows the phase diagram on $\lambda - a$ plane for (a) $\alpha = 0.1$ and (b) $\alpha = 0.5$. The range of parameters that gives RS phase shrinks as α decreases. The conventional value $a = 3.7$ [4], which is indicated by horizontal lines in Figure 7, is considered as one of the appropriate value of a to obtain RS stability at sufficiently large λ . As decrease λ , the value of a to achieve RS phase diverges, which is consistent with the shape of SCAD regularization.

Figure 8 shows the parameter dependence of the sparsity ρ/α in the RS phase. The sparsity is almostly controlled by λ ; as increase λ , the non-zero components in the

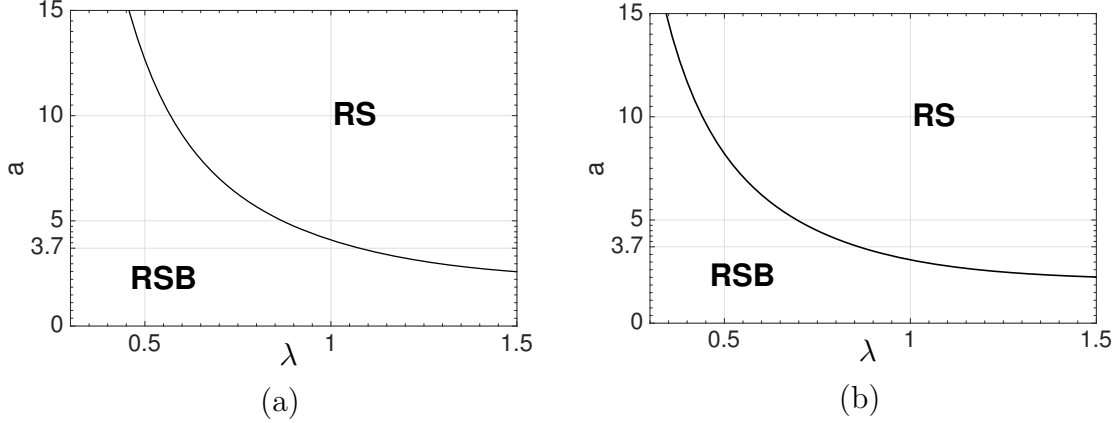


Figure 7. Phase diagram of $a - \lambda$ plane at (a) $\alpha = 0.1$ and (b) $\alpha = 0.5$. The conventional value $a = 3.7$ is indicated by the horizontal dashed lines.

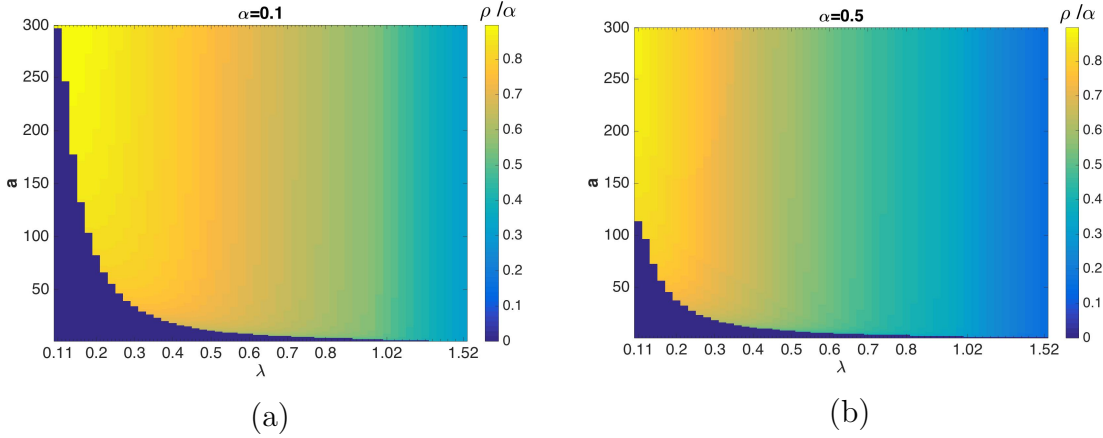


Figure 8. Parameter dependence of the sparsity at (a) $\alpha = 0.1$ and (b) $\alpha = 0.5$ in the RS phase. The figures were created by presenting the elements of matrix $\rho(a, \lambda)/\alpha$ in color map, which cause the block like shapes.

estimate is enhanced. The sparsity slightly depends on a compared with λ , but as a decreases, the number of non-zero components increases. This fact is reasonable from the form of the regularization, because the gradient around the origin that is a key of the sparsity is governed by λ .

As the number of non-zero component decreases, the representation performance of data is generally decreased. There is a trade-off relationship between the simplicity and the accuracy of the expression. We quantify this relationship by regarding the representation error (101) as a function of sparsity ρ/α . Here, ρ/α corresponds to the ratio of the number of variables to be estimated and that of known variables, and hence $\rho/\alpha \leq 1$ is the physically meaningful region. As mentioned in Sec.4 and explained in Appendix A, the representation error is given by $\hat{\chi}$ in replica method, and hence we obtain the dependency of the representation error on the sparsity by solving (87) and (98).

Figure 9 show the representation error as a function of the sparsity at $\alpha = 0.5$ and

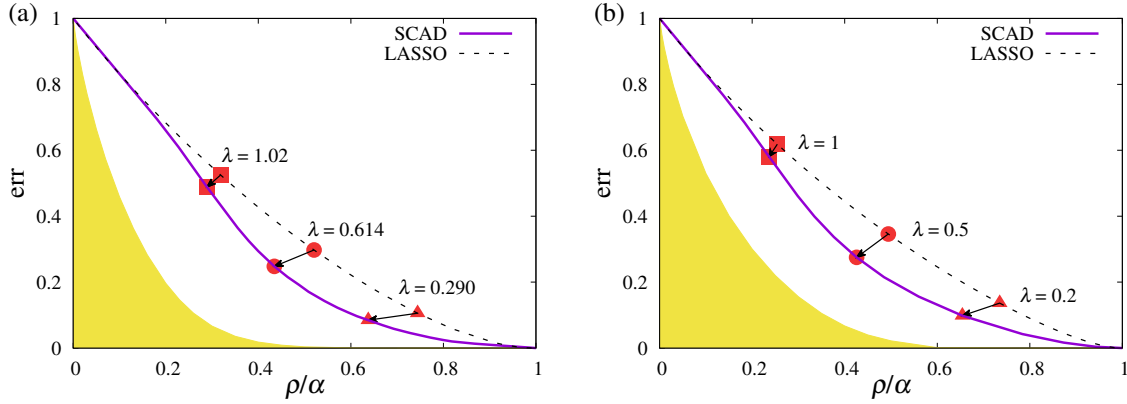


Figure 9. Relationship between representation error and the normalised sparsity ρ/α for (a) $\alpha = 0.5$ and (b) $\alpha = 0.8$. LASSO corresponds to $a \rightarrow \infty$ limit, and the shift of the error curve by decreasing a is indicated by arrows. The shaded regions are not achievable region for any compression method [30].

$\alpha = 0.8$. For comparison, the results obtained by ℓ_1 regularization, which corresponds to $a \rightarrow \infty$, are shown by dashed lines, and not achievable region for any estimation method [30] are shaded. At each value of λ , we find the value of a that gives the smallest representation error. The shift of the representation error curve associated with the decrease of a are shown by arrows in Figure 9, where the minimum values of a are (a) $a = 3, 6, 20$, for $\lambda = 0.290, 0.614, 1.02$, respectively, and (b) $a = 2.739, 6.51, 25$, for $\lambda = 0.2, 0.5, 1$, respectively. The representation error monotonically decreases as a decreases, and hence when we restrict the SCAD parameters to be within the replica symmetric region, the smallest representation error is obtained at the RS/RSB boundary. In addition, the sparsity slightly decreases as a decreases, and hence the sparsest and accurate expression is obtained by decreasing a to be on the RS/RSB boundary.

6. Correspondence between RS/RSB transition and convergence of coordinate descent: a conjecture

For SCAD penalty, it is shown that coordinate descent (CD) algorithm is valid at a certain parameter region[5]. CD is the component-wise minimization of energy density (6), while all other components are fixed, cycling through all parameters until convergence is reached. Let us denote the estimates at step t of CD as $\hat{\mathbf{x}}^{(t)}$ and define the residue at step 0 as $\mathbf{r}^{(0)} = \mathbf{y} - \mathbf{A}\hat{\mathbf{x}}^{(0)}$. CD for SCAD is given by the cyclic update of one component of the estimates $\hat{\mathbf{x}}$ according to the following equations: [5]

$$z_j^{(t+1)} = \mathbf{A}_j^T \mathbf{r}^{(t)} + \hat{x}_j^{(t)} \quad (105)$$

$$\hat{x}_j^{(t+1)} = \begin{cases} S(z_j^{(t+1)}, \lambda) & \text{for } |z_j^{(t+1)}| \leq 2\lambda \\ \frac{S(z_j^{(t+1)}, a\lambda/(a-1))}{1 - (a-1)^{-1}} & \text{for } 2\lambda < |z_j^{(t+1)}| \leq a\lambda \\ z_j^{(t+1)} & |z_j^{(t+1)}| > a\lambda \end{cases} \quad (106)$$

$$\mathbf{r}^{(t+1)} = \mathbf{r}^{(t)} - (\hat{x}_j^{(t+1)} - \hat{x}_j^{(t)})\mathbf{A}_j, \quad (107)$$

where S is the soft-thresholding function defined by

$$S(z, \lambda) = \begin{cases} z - \text{sign}(z)\lambda & \text{for } |z| > \lambda \\ 0 & \text{otherwise} \end{cases}, \quad (108)$$

and \mathbf{A}_j denotes j -th column vector of \mathbf{A} . A sufficient condition for the convergence of the coordinate descent to the globally stable state is proposed as [5]

$$a > 1 + c(\lambda, a; \mathbf{A})^{-1}. \quad (109)$$

Here $c(\lambda, a; \mathbf{A})$ is the minimum eigenvalue of the Gram matrix $\mathbf{A}_{S(\lambda, a)}^T \mathbf{A}_{S(\lambda, a)}$, where $S(\lambda, a)$ is the union of the support at λ and the index of a component in \mathbf{x} which will become nonzero at $\lambda - d\lambda$. The infinitesimal amount $d\lambda (> 0)$ is set such that the difference between the numbers of the support at λ and $\lambda - d\lambda$ becomes 1. However, the sufficient and necessary condition for the convergence of CD is not known. We suggest here that the convergence condition of CD and AMP are equivalent from numerical observation.

To check the convergence of the CD, we prepare m random initial conditions for CD. The fixed point of CD started from k -th initial condition under the fixed data \mathbf{y} and predictor matrix \mathbf{A} is denoted as $\hat{\mathbf{x}}_k^{\text{CD}}(\mathbf{y}, \mathbf{A})$. We compute the average of the differences between the fixed points as

$$d(\mathbf{y}, \mathbf{A}) = \frac{1}{\frac{m(m-1)}{2}} \sum_{k < l} \|\hat{\mathbf{x}}_k^{\text{CD}}(\mathbf{y}, \mathbf{A}) - \hat{\mathbf{x}}_l^{\text{CD}}(\mathbf{y}, \mathbf{A})\|_2^2. \quad (110)$$

The uniqueness of the stable solution for CD is indicated by $d(\mathbf{y}, \mathbf{A}) = 0$. We define $a^*(\mathbf{y}, \mathbf{A}; \lambda)$ as the minimum value of a that satisfy $d(\mathbf{y}, \mathbf{A}) = 0$ for each λ , in other words, at $a < a^*(\mathbf{y}, \mathbf{A}; \lambda)$, CD is not always attained to the global minimum. In Figure 10, the averaged value of $a^*(\mathbf{y}, \mathbf{A}; \lambda)$, which means typical solvable limit, over 100 samples of i.i.d. Gaussian random \mathbf{y} and \mathbf{A} are shown by circles \circ for (a) $N = 200$, $M = 20$ ($\alpha = 0.1$), (b) $N = 200$, $M = 50$ ($\alpha = 0.5$), where we set $m = 100$. In comparison, we show the convergence condition (109) averaged over the same \mathbf{y} and \mathbf{A} by squares \square , and RS/RSB boundary (104). As shown in Figure 10, RS/RSB transition is an approval indicator of the convergence of CD, although the complete correspondence between them has not been mathematically proved. From the physical consideration, RS/RSB transition is supposed to correspond to the appearance of the local minimums whose number is exponential order of the system size. This picture of the RS/RSB transition is consistent with the result shown in Figure 10.

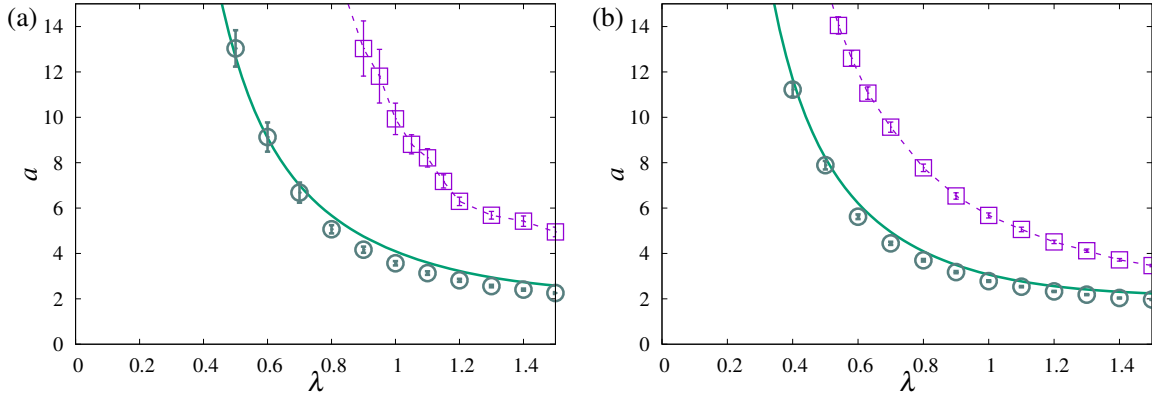


Figure 10. Comparison between AT lines (solid lines) and typically solvable limit of CD (denoted by \circ) for (a) $N = 200$, $M = 20$ ($\alpha = 0.1$) and (b) $N = 200$, $M = 100$ ($\alpha = 0.5$). The sufficient condition for the convergence of CD are shown by solid lines with \square .

7. Summary and conclusion

We have studied a linear regression problem under SCAD regularization. We have developed AMP for SCAD regularization, and identified the stability condition of AMP's fixed point. This stability condition corresponds to AT condition derived by replica method, and the correspondence between the stability of AMP and that of RS solution has been indicated. The stability analysis does not depend on the form of the regularization, and hence the correspondence holds for other regularizations that exhibits RS/RSB transition. In addition, we have identified the replica symmetric phase on the $\lambda - a$ parameters plane, and quantify the relationship between the representation error and the sparsity. We have theoretically showed that, for i.i.d. Gaussian data and basis matrix, SCAD regularization typically provides more accurate and sparser expression compared with ℓ_1 regularization in RS phase. Furthermore, the smallest representation error is obtained at the RS/RSB boundary for each λ .

Our result shows that the nonconvexity of the sparse regularization does not always provide instability of the replica symmetry, and possibilities of message passing algorithms for nonconvex regularizations. Since the unclear condition of global stability is the main concern for nonconvex sparse regularization in practice, identifying and utilizing the RS region of other nonconvex sparse regularization is a valid potential future work. In this paper, we have focused on the case that data \mathbf{y} and predictor matrix \mathbf{A} are i.i.d. Gaussian random variables. Our discussion is applicable for non-Gaussian \mathbf{A} and \mathbf{y} that satisfying following conditions: the correlation between components are negligible, each component of \mathbf{A} have zero mean and variance $1/M$, and each component of \mathbf{y} are zero mean and variance σ_y^2 . However, in dealing with general data, non-zero mean might be considered. Our algorithm is still applicable for such cases introducing a simple modification that lead zero mean matrix and vector as $\mathbf{y} - \bar{\mathbf{y}} = (\mathbf{A} - \bar{\mathbf{A}})\mathbf{x}$, where $\bar{\mathbf{y}} \equiv (\frac{1}{M} \sum_{\mu} y_{\mu})\mathbf{1}$, $\mathbf{1}$ denotes the M dimensional identity vector and $\bar{\mathbf{A}}$ is the $M \times N$

matrix where the i -th column is given by the values $\bar{A}_i \equiv (1/M) \sum_{\mu} A_{\mu i}$. For more general case where the correlation between components of \mathbf{A} and \mathbf{y} is not negligible, the convergence of AMP and the validness of approximations introduced into AMP would be a problem to be resolved. Incorporation of nonconvex regularization into variants of AMP [31] where the convergence is improved, is useful for further discussion.

Acknowledgments

The authors would like to thank Yoshiyuki Kabashima for insightful discussions and comments. This work is supported by JSPS KAKENHI No.16K16131 and Shiseido Female Researcher Science Grant (AS), and by the Academy of Finland through its Center of Excellence COIN (YX).

Appendix A. Replica method for SCAD regularization

Assuming that n is an integer, we can express the expectation of Z_{β}^n in (82) by using n -replicated systems;

$$E_{\mathbf{y}, \mathbf{A}}[Z_{\beta}^n(\mathbf{y}, \mathbf{A})] = \int d\mathbf{A} d\mathbf{y} P_{A, \mathbf{y}}(\mathbf{A}, \mathbf{y}) \int d\mathbf{x}^{(1)} \dots d\mathbf{x}^{(n)} \times \exp \left[\sum_{b=1}^n \left\{ -\frac{\beta}{2} \|\mathbf{y} - \mathbf{A}\mathbf{x}^{(b)}\|_2^2 - \beta J_{\lambda, a}(\mathbf{x}^{(b)}) \right\} \right] \quad (\text{A.1})$$

The microscopic states of $\{\mathbf{x}^{(b)}\}$ are characterized by the macroscopic quantities

$$q^{(bc)} = \frac{1}{N} \sum_i x_i^{(b)} x_i^{(c)}, \quad (\text{A.2})$$

which is defined for all combinations of replica indices b and c ($b \geq c$). By introducing the identity

$$1 = \int dq^{(bc)} \delta \left(q^{(bc)} - \frac{1}{M} \sum_i x_i^{(b)} x_i^{(c)} \right) \quad (\text{A.3})$$

for all combinations of (b, c) , the following expression is obtained after the integration with respect to \mathbf{A} :

$$E_{\mathbf{y}, \mathbf{A}}[Z_{\beta}^n(\mathbf{y}, \mathbf{A})] = \int d\mathcal{Q} \mathcal{S}(\mathcal{Q}) \mathcal{I}(\mathcal{Q}) \quad (\text{A.4})$$

where the function $\mathcal{S}(\mathcal{Q})$ and \mathcal{I} are given by

$$\mathcal{S}(\mathcal{Q}) = \int d\hat{\mathcal{Q}} \{d\mathbf{x}^{(b)}\} \exp \left\{ -M \sum_{b \leq c} q^{(bc)} \hat{q}^{(bc)} + \sum_{b \leq c} \sum_i \hat{q}^{(bc)} x_i^{(b)} x_i^{(c)} - \beta \sum_{b=1}^n J_{\lambda, a}(\mathbf{x}^{(b)}) \right\}, \quad (\text{A.5})$$

$$\mathcal{I}(\mathcal{Q}) = \int \{d\mathbf{u}^{(b)}\} P_u(\{\mathbf{u}^{(b)}\} | \mathcal{Q}) \int d\mathbf{y} P_y(\mathbf{y}) \exp \left\{ -\frac{\beta}{2} \sum_{b=1}^n \|\mathbf{y} - \mathbf{u}^{(b)}\|_2^2 \right\} \quad (\text{A.6})$$

The $n \times n$ matrices \mathcal{Q} and $\hat{\mathcal{Q}}$ are the matrix representations of $\{q^{(bc)}\}$ and $\{\hat{q}^{(bc)}\}$, respectively, where $\{\hat{q}^{(bc)}\}$ are conjugate variables for the representation of the delta function in (A.3). Each component of $\mathbf{u}^{(b)} \in \mathbb{R}^M$, denoted by $u_\mu^{(b)}$, is statistically equivalent to $\sum_i A_{\mu i} x_i^{(b)}$. The probability distribution of $\{\mathbf{u}^{(b)}\}$ is given by the product of the Gaussian distribution with respect to the vector $\tilde{\mathbf{u}}_\mu = \{u_\mu^{(1)}, \dots, u_\mu^{(n)}\}$ such as [25]

$$P_u(\{\mathbf{u}^{(b)}\}|\mathcal{Q}) = \prod_{\mu=1}^M \frac{1}{\sqrt{(2\pi)^n |\mathcal{Q}|}} \exp\left(-\frac{1}{2} \tilde{\mathbf{u}}_\mu^T \mathcal{Q}^{-1} \tilde{\mathbf{u}}_\mu\right). \quad (\text{A.7})$$

To obtain an analytic expression with respect to $n \in \mathbb{R}$ and take the limit as $n \rightarrow 0$, we restrict the candidates for the dominant saddle point to those of RS form as

$$(q^{(bc)}, \hat{q}^{(bc)}) = \begin{cases} (Q, -\tilde{Q}/2) & (b = c) \\ (q, \tilde{q}) & (b \neq c). \end{cases} \quad (\text{A.8})$$

Under the RS assumption (A.8), we obtain

$$\begin{aligned} \mathcal{S}(Q, q) = \int d\tilde{Q} d\tilde{q} \exp \left[M \left\{ \frac{-nQ\tilde{Q} + n(n-1)q\tilde{q}}{2} \right. \right. \\ \left. \left. + \log \int Dz \left(\int dx \exp \left(\frac{\tilde{Q}}{2} x^2 + \sqrt{\tilde{q}} z - \beta J_{\lambda,a}(x) \right) \right)^n \right\} \right] \end{aligned} \quad (\text{A.9})$$

$$\mathcal{I}(Q, q) = \{(1 + \beta(Q - q))^{n-1} (1 + \beta Q + \beta(n-1)q)\}^N \quad (\text{A.10})$$

For $\beta \rightarrow \infty$, RS order parameters scale to keep $\beta(Q - q) = \chi$, $\beta^{-1}(\tilde{Q} + \tilde{q}) = \hat{Q}$, and $\beta^{-2}\tilde{q} = \hat{\chi}$ of the order of unity. The integral with respect to x in (A.9) is processed by saddle point method at $\beta \rightarrow \infty$ that corresponds to the single-body problem of the estimate (92). Substituting (A.4) (A.9), and (A.10) into (82), we obtain the RS free energy density (83).

The free energy density corresponds to the minimum value of energy. Therefore, one can derive the representation error (101) by discarding the expectation of the regularization term from the free energy density as

$$\text{err} = 2 \left(f - \frac{1}{M} E_{\mathbf{y}, \mathbf{A}} [J_{\lambda,a}(\hat{\mathbf{x}}(\mathbf{y}, \mathbf{A}))] \right). \quad (\text{A.11})$$

As mentioned in Sec.4, x^* is statistically equivalent to the solution of the original problem, and hence the expectation value of the regularization term is derived as

$$\lim_{N \rightarrow \infty} \frac{1}{M} E_{\mathbf{y}, \mathbf{A}} [J_{\lambda,a}(\hat{\mathbf{x}}(\mathbf{y}, \mathbf{A}))] = \frac{1}{\alpha} \int Dz J_{\lambda,a}(x^*(z; \hat{Q}, \hat{\chi})). \quad (\text{A.12})$$

Substituting the expression of (A.12) under RS assumption into (A.11), the relationship $\hat{\chi} = \text{err}$ is obtained.

Appendix B. Derivation of de Almeida-Thouless condition

The local stability of RS solution against symmetry breaking perturbation is examined by constructing 1 replica symmetry breaking (RSB) solution. We introduce 1RSB

assumption with respect to the saddle point as

$$(q^{(bc)}, \hat{q}^{(bc)}) = \begin{cases} (Q, -\tilde{Q}/2) & (b = c) \\ (q_1, \tilde{q}_1) & (b \neq c, B(b) = B(c)) \\ (q_0, \tilde{q}_0) & (B(b) \neq B(c)) \end{cases}, \quad (\text{B.1})$$

where n replicas are separated into \tilde{l} blocks that contain n/\tilde{l} replicas. The index of block that b -th replica is included is denoted by $B(b)$. At $\beta \rightarrow \infty$, these 1RSB order parameters scale as $\beta(Q - q_1) = \chi$, $\beta^{-1}(\tilde{Q} + \tilde{q}_1) = \hat{Q}$, $\beta^{-2}\tilde{q}_1 = \hat{\chi}_1$, $\beta^{-2}\tilde{q}_0 = \hat{\chi}_0$, and $\tilde{l} = l/\beta$. Following the similar calculation explained in Appendix A, the free energy density under 1RSB assumption is derived as

$$f = \frac{\alpha(Q + \sigma_y^2)}{2\{1 + \chi + l(Q - q_0)\}} - \frac{\alpha(\hat{Q}Q - \hat{\chi}_1\chi)}{2} + \frac{\alpha l(\hat{\chi}_1Q - \hat{\chi}_0q_0)}{2} - \frac{1}{l} \int Dz \log \Xi + \frac{\alpha}{2l} \log \left(1 + \frac{l(Q - q_0)}{1 + \chi} \right) \quad (\text{B.2})$$

where

$$\Xi = \int Dw \exp(lf_\xi^*) \quad (\text{B.3})$$

$$f_\xi^* = \min_x f_\xi(x) \quad (\text{B.4})$$

$$f_\xi(x) = \frac{\hat{Q}}{2}x^2 - (\sqrt{\hat{\chi}_1}z + \sqrt{\hat{\chi}_1 - \hat{\chi}_0}w)x + J_{\lambda,a}(x). \quad (\text{B.5})$$

We denote the minimizer of (B.4) as x_{RSB}^* . The saddle point equations are given by

$$\hat{Q} = \frac{1}{1 + \chi} \quad (\text{B.6})$$

$$\hat{\chi}_1 = \frac{Q - q_0}{(1 + \chi)(1 + \chi + l(Q - q_0))} + \hat{\chi}_0 \quad (\text{B.7})$$

$$\hat{\chi}_0 = \frac{Q + \sigma_y^2}{(1 + \chi + l(Q - q_0))^2} \quad (\text{B.8})$$

$$Q = \frac{1}{\alpha} \int Dz \langle x_{\text{RSB}}^{*2} \rangle_w \quad (\text{B.9})$$

$$\chi = \frac{1}{\alpha} \int Dz \left\langle \frac{\partial x_{\text{RSB}}^*}{\partial (\sqrt{\hat{\chi}_1 - \hat{\chi}_0}w)} \right\rangle_w \quad (\text{B.10})$$

$$q_0 = \frac{1}{\alpha} \int Dz \langle x_{\text{RSB}}^* \rangle_w^2, \quad (\text{B.11})$$

where

$$\langle g(w) \rangle_w = \frac{\int Dw \exp(lf_\xi^*) g(w)}{\int Dw \exp(lf_\xi^*)} \quad (\text{B.12})$$

with an arbitrary function $g(w)$. When $q_0 = Q$ and $\hat{\chi}_0 = \hat{\chi}_1$, 1RSB solution is reduced to RS solution, and hence the stability of RS solution is examined by the stability analysis of the 1RSB solution of $Q = q_0$ and $\hat{\chi}_1 = \hat{\chi}_0$. We define $\Delta = Q - q_0$ and $\hat{\Delta} = \hat{\chi}_1 - \hat{\chi}_0$, and apply Taylor expansion to them assuming that they are sufficiently small. From

(B.7) and (B.8), we obtain

$$\hat{\Delta} = \frac{1}{(1 + \chi)^2} \Delta + O(\Delta^2). \quad (\text{B.13})$$

For the expansion of Δ around $\hat{\Delta} = 0$, the saddle point equations for finite β is useful, which are obtained by replacing x_{RSB}^* with

$$\langle x \rangle = \frac{\int dx x \exp(\beta f_\xi)}{\int dx \exp(\beta f_\xi)}, \quad (\text{B.14})$$

and $\langle g(w) \rangle_w$ for finite β is defined by

$$\langle g(w) \rangle_w = \frac{\int Dw \left\{ \int dx \exp(\beta f_\xi) \right\}^{\bar{l}} g(w)}{\int Dw \left\{ \int dx \exp(\beta f_\xi) \right\}^{\bar{l}}} \quad (\text{B.15})$$

because these expression depends on $\hat{\Delta}$ only through f_ξ . Differentiating $Q - q_0$ by $\hat{\Delta}$ at $\hat{\Delta} = 0$, we obtain

$$\left. \frac{\partial \Delta}{\partial \hat{\Delta}} \right|_{\hat{\Delta} \rightarrow 0} = \frac{\beta^2}{\alpha} \int Dz \left\{ \langle x^2 \rangle^2 - 2 \langle x^2 \rangle \langle x \rangle^2 + \langle x \rangle^4 \right\}, \quad (\text{B.16})$$

which is equivalent to

$$\left. \frac{\partial \Delta}{\partial \hat{\Delta}} \right|_{\hat{\Delta} = 0} = \frac{1}{\alpha} \int Dz \left(\frac{\partial x^*}{\partial \sqrt{\hat{\chi}} z} \right)^2 \quad (\text{B.17})$$

at $\beta \rightarrow \infty$. Substituting (B.17) into (B.13), we get

$$\hat{\Delta} = \frac{1}{\alpha} \int Dz \left(\frac{\partial x^*}{\partial \sqrt{\hat{\chi}} z} \right)^2 \hat{\Delta} + O(\hat{\Delta}^2), \quad (\text{B.18})$$

which means that the local stability of $\hat{\Delta} = 0$ is lost when

$$\frac{1}{\alpha} \int Dz \left(\frac{\partial x^*}{\partial \sqrt{\hat{\chi}} z} \right)^2 > 1. \quad (\text{B.19})$$

This is de Almeida-Thouless condition for the current problem.

References

- [1] Breiman, L, 1996, *The annals of statistics*, **24**, 2350.
- [2] Tibshirani R 1996 *J. Roy. Statist. Soc. Ser. B* **58** 267
- [3] Zhang C-H, 2010, *The Annals of Statistics*, **38**, 894.
- [4] Fan J and Li R 2001 *J. Amer. Statist. Assoc.* **96** 1348
- [5] Breheny P and Huang J, 2011 *The Annals of Applied Statistics*, **5**, 232–253.
- [6] Frank, L E and Friedman, J H, 1993 *Technometrics*, **35**, 109–135.
- [7] Horel A E and Kennard R W, 1970 *Technometrics*, **12**, 55–67.
- [8] Donoho D 2006 *IEEE Trans. Inform. Theory* **52** 1289
- [9] Huang J and Xie H, *Asymptotic oracle properties of SCAD-penalized least squares estimators*, in *Asymptotics: Particles, Processes and Inverse Problems*, Institute of Mathematical Statistics, (2007), 149–166.
- [10] Kim Y, Choi H and Oh H-S, 2008, *Journal of the American Statistical Association*, **103**, 1665–1673
- [11] Natarajan B K, 1995, *SIAM journal on computing*, **24**, 227.
- [12] Mézard M, Parisi G and Virasoro M 1987 *Spin Glass Theory and Beyond* (World Scientific)

- [13] Mézard M and Montanari A 2009 *Information, Physics, and Computation* (Oxford: Oxford Press)
- [14] MacKay D JC 1999 *IEEE transactions on Information Theory*, **45** 399–431.
- [15] Kabashima Y and Saad D 1998 *EPL*, **44**, 668
- [16] Donoho D L, Maleki A and Montanari A 2009 *Proc. Nat. Acad. Sci. USA* **106** 18914
- [17] Donoho D L, Maleki A and Montanari A 2011 *IEEE Trans. Inf. Theory* **57** 6920
- [18] Montanari A and Bayati M, 2011 *IEEE Transaction on Information Theory*, **57**, 764–785.
- [19] Rangan S 2011 in *Proceedings of the 2011 IEEE International Symposium on Information Theory Proceedings (ISIT), Austin, Texas* (IEEE, New York), 2168
- [20] Xu Y, Kabashima Y and Zdeborová L, 2014 *J Stat Mech.* **2014**, P11015
- [21] Thouless D J and Anderson P W and Palmer R G, 1997 *Philosophical Magazine*, **35**, 593–601
- [22] Shiino M and Fukai T, 1992 *J. Phys. A: Math. Gen.* , **25**, L375
- [23] Krzakala F, Mézard M, Sausset F, Sun Y F and Zdeborova L 2012 *Phys. Rev. X* **2** 021005
- [24] Kabashima Y 2003 *J. Phys. A*, **36**, 11111–11121.
- [25] Kabashima Y, Wadayama T and Tanaka T 2009 *J. Stat. Mech.* L09003
- [26] Sakata A, 2016, *J. Stat. Mech.*, **2016**, 123302
- [27] Xu Y and Kabashima Y, 2016 *J. Stat. Mech.*, **2016**, 083405
- [28] Xu Y and Kabashima Y 2013 *J. Stat. Mech.*, **2013**, P02041
- [29] de Almeida J R L and Thouless D J 1978 *J. Phys. A: Math. Gen.* **11** 983
- [30] Nakanishi-Ohno Y, Obuchi T, Okada M and Kabashima Y 2016 *J. Stat. Mech.* **2016** 063302
- [31] Schniter P, Rangan S and Fletcher A K, 2017 *Information Theory Proceedings (ISIT), 2017 IEEE International Symposium on*, 1588